

Supporting Information:

Single-Molecule Fluorescence Lifetime Imaging Using Wide-Field and Confocal-Laser Scanning Microscopy: a Comparative Analysis

Nazar Oleksiiievets,^{†,||} Christeena Mathew,^{‡,||} Jan Christoph Thiele,[†] Jose Ignacio Gallea,[†] Oleksii Nevskiy,[†] Ingo Gregor,[†] André Weber,[¶] Roman Tsukanov,^{*,†} and
Jörg Enderlein^{*,†,§}

[†]*III. Institute of Physics – Biophysics, Georg August University, 37077 Göttingen,
Germany.*

[‡]*Laboratory of Supramolecular Chemistry, EPFL SB ISIC LCS, BCH 3307, CH-1015
Lausanne, Switzerland.*

[¶]*Combinatorial NeuroImaging Core Facility, Leibniz Institute for Neurobiology,
Brenneckestraße 6, 39118 Magdeburg, Germany.*

[§]*Cluster of Excellence “Multiscale Bioimaging: from Molecular Machines to Networks of
Excitable Cells” (MBExC), Georg August University, Göttingen, Germany.*

|| These authors contributed equally to this work

E-mail: rtsukan@gwdg.de; jenderl@gwdg.de

Wide-field and confocal FLIM optical setups

Wide-field FLIM setup

Wide-field measurements were performed using a custom-built optical setup, as described elsewhere,^{S1} and shown in Figure S1a. Pulsed super-continuum white light laser (Fianium WhiteLase SC450, NKT Photonics) with a pulse repetition of 20 MHz was used for excitation. The TCSPC-based camera was optically triggered using a custom-built photodiode (PD). A clean-up filters (ZET 640/10, Chroma; BrightLine HC 563/9, Semrock; ZET 488/10, Chroma) were positioned in front of the white light laser output to excite in different wavelengths. Neutral density filters (NE10A-A, NE20A-A, Thorlabs), and the variable neutral density filter (ND) (NDC-50C-4-A, Thorlabs) were used to adjust the laser excitation power. The laser beam was coupled into a single-mode optical fiber (P1-460B-FC-2, Thorlabs) with a typical coupling efficiency of 40%. After exiting the optical fiber, the collimated laser beam was expanded by a factor of $3.6 \times$ using telescope lenses (TL1 and TL2). The typical excitation intensity at the sample was $10\text{--}20 \text{ W/cm}^2$.

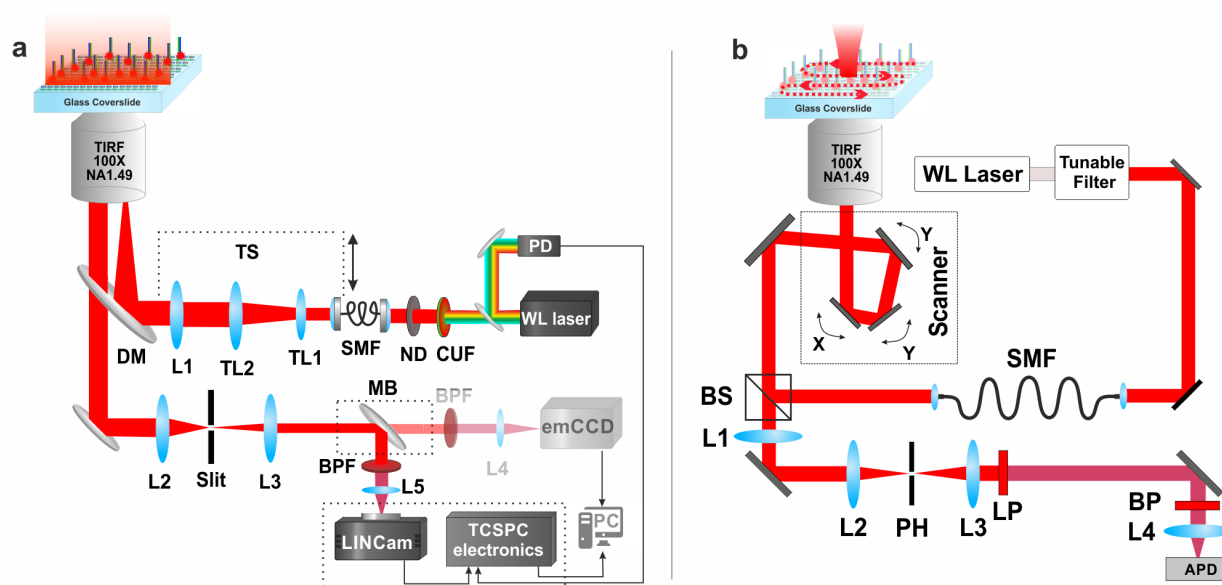


Figure S1: FLIM setups. Schematic representation of the custom-built wide-field FLIM setup equipped with lifetime camera (a) and time-resolved confocal FLIM setup equipped with fast scanner (b).

The laser beam was focused onto the back focal plane of the TIRF objective (UAPON 100 \times oil, 1.49 NA, Olympus) using achromatic lens (L1) (AC508-180-AB, Thorlabs). Mechanical shifting of the beam with respect to the optical axis was done through a translation stage TS (LNR25/M, Thorlabs) for switching between EPI, HILO, and TIR illumination schemes. The smooth lateral sample positioning was achieved by using a high-performance two-axis linear stage (M-406, Newport). In addition, an independent one-dimensional translation stage (LNR25/M, Thorlabs) together with a differential micrometer screw (DRV3, Thorlabs) was used to move the objective along the optical axis for focusing. The spectral separation of the collected fluorescence light from the excitation pathway was achieved using a multi-band dichroic mirror DM (Di03 R405/488/532/635, Semrock), which direct the fluorescence light towards the tube lens L2 (AC254-200-A-ML, Thorlabs). The field of view was physically limited in the emission path by an adjustable slit aperture (SP60, OWIS) positioned in the image plane in order to image a region with a uniform excitation intensity distribution and also to limit the photon flux reaching the lifetime camera. Lenses L3 (AC254-100-A, Thorlabs) and L4 (AC508-150-A-ML, Thorlabs) re-imaged the emitted fluorescence light from the slit onto an emCCD camera (iXon Ultra 897, Andor). Similarly, lens L5 (AC508-250-A-MC, Thorlabs) re-imaged the light onto the lifetime camera (LINCam25, Photonscore). The switching between the two cameras is attained by using a dielectric mirror (BB1-E02, Thorlabs) positioned on a magnetic base plate MB (KB50/M, Thorlabs) with removable top. A band-pass filters BP (BrightLine HC 692/40, Semrock; BrightLine HC 615/45, Semrock; BrightLine FF 536/40, Semrock) were used to block the scattered excitation light. The total magnification on the emCCD camera was 166.6 \times , resulting in an effective pixel size in the sample space of 103.5 nm. The total magnification for imaging with TCSPC-based camera was 222 \times , resulting in the partitioning of the field of view into 1024 \times 1024 pixels with the effective pixel size in sample space of 95.8 nm. All experiments were done at $22 \pm 1^\circ\text{C}$. This was crucial for the mechanical stability of the optical setup used.

Confocal FLIM setup

Fluorescence lifetime measurements were performed on a custom-built confocal microscopy setup as described previously,^{S2} see Figure S1b. For the excitation in 640 nm wavelength 40 MHz pulsed diode laser (PDL 800-B driver with LDH-D-C-640 diode, PicoQuant) was used, for the excitation in 488 nm 40 MHz pulsed diode laser (PDL 800-B driver with LDH-D-C-488 diode, PicoQuant) was employed and for the excitation in 560 nm white light laser (Fianium WhiteLase SC450, NKT Photonics) was used. The laser beam was coupled into a single-mode fiber (PMC-460Si-3.0-NA012 3APC-150-P, Schafter+Kirchhoff) using a fiber-coupler (60SMS-1-4- RGBV-11-47, Schafter+Kirchhof). The laser was decoupled from the fiber and collimated using 10× air objective (UPlanSApo 10× /0.40 NA, Olympus). After passing thorough a clean-up filter (MaxDiode 640/8, Semrock or BrightLine HC 563/9, Semrock or ZET 488/10, Chroma), the quad-band dichroic mirror (ZT405/488/561/640rpc, Chroma) was used to direct the excitation light into the specimen and to decouple it from the emission light.

The excitation beam passed through a fast laser scanning system (FLIMbee, PicoQuant). The scanning system was used to deflect the beam, while preserving the laser focus position in the back focal plane of the objective (UApo N 100×/1.49 NA oil, Olympus). The region of interest and the focus plane were controlled by the manual XY stage (Olympus) and a z-piezo stage (Nano-ZL100, MadCityLabs), respectively. The emitted fluorescence light was collected by using the same objective as used for the excitation and sample scan. The emission light was focused onto the pinhole with 100 nm diameter (P100S, Thorlabs) using 180 mm achromatic lens (TTL180-A, Thorlabs). The long-pass filter (647 LP Edge Basic, Semrock) was used to block the excitation laser light in the emission path. followed by the emission light was collimated by a 100 mm lens. A band-pass filter (BrightLine HC 692/40, Semrock or BrightLine HC 615/45, Semrock or BrightLine FF 536/40, Semrock) was used to reject the scattered excitation light. Finally, the emission light was focused onto a SPAD-detector (SPCM-AQRH, Excelitas) with the achromatic lens (AC254030-A-ML, Thorlabs).

Dark count rate of the detector was less than 150 counts per second. The output signal of the photon detector was recorded using a TCSPC system (HydraHarp 400, PicoQuant). Data was acquired using a commercial software from Picoquant (SymPhoTime 64, PicoQuant), which controlled both the TCSPC and the scanner systems. For CLSM-based FL-SMLM, ROIs of $20 \times 20 \mu\text{m}^2$ size were scanned. Typically, 10 sample scans with a virtual pixel size of 100 nm, and a dwell time of 100 $\mu\text{s}/\text{pixel}$ were chosen. Typical FL-SMLM movie acquisition times varied between 3 and 5 minutes. Localization events containing more than 100 photons and less than 5000 photons were taken into account.

FL-SMLM/MIET-SMLM imaging

FL-SMLM sample preparation: DNA-assisted surface immobilization of single fluorophores

We used double-stranded DNA (dsDNA) to immobilize different fluorophores on a surface. This dsDNA-assisted immobilization of fluorophores does also create favorable photophysical conditions for fluorophores. One strand of the dsDNA carried a biotin on its 5' end: 5' \rightarrow 3', Biotin - AATCGATGATAGACGTTGTGGCTGC. The second complementary strand was labeled on its 3' end with a fluorophore: 5' \rightarrow 3', GCAGCCACAACGTCTATCATCGATT-fluorophore. The two DNA strands were annealed together to form dsDNA by first heating up to 94°C at ~ 200 nM concentration for both single strands for 5 min and then gradually cooling down to room temperature within 30 min. The obtained dsDNA construct was stable for several weeks. The dsDNA molecule was designed in such a way that after immobilization via the biotin to surface-attached neutravidin, the fluorophore faced the coverslip surface and therefore decreased the linkage error by shortening the distance between fluorophore and surface anchor point. The sample itself were prepared from glass coverslips that were cleaned by sonicating in KOH solution (1M concentration) for 15 min, rinsed with doubly distilled water for at least 3 times and dried using air flow. Then, four-wells silicone

inserts (Ibidi 80469, Germany) were attached to the coverslips. DNA-fluorophore molecules were immobilized to the surface using biotin-avidin chemistry. For surface passivation, the following procedure was used: BSA-biotin (A8549, Sigma-Aldrich) was diluted in 10 mM Tris and 50 mM NaCl (buffer A, pH 8.0) to a concentration of 0.5 mg/mL, injected into a chamber, and incubated overnight at 4°C. Afterwards, the chamber was flushed with buffer A for at least 3 times. Neutravidin (31000, Thermo Fisher Scientific) was diluted in buffer A to a concentration of 0.5 mg/mL, and then injected into a chamber and incubated for 5 min. Next, the chamber was flushed with buffer A for at least 3 times. Then, a solution containing labeled DNA molecules (~ 500 pM concentration) was injected into a chamber and incubated for a few minutes, until sufficient surface coverage with fluorescently labeled dsDNA was achieved. Then, the chamber was flushed with buffer A and imaged. Typical acquisition time was few minutes, depending mostly upon photobleaching rate. For all samples, intensity time traces were examined and single-step photobleaching was used to check that indeed single molecules with sufficient distance in between were immobilized.^{S3} The thickness of the biotin-avidin immobilization layer is known to be ~ 12 nm^{S4} and it was taken into account in the total height estimation of a fluorophore above the coverslip surface in the MIET-SMLM experiments, see below.

Buffer solutions

Following buffers were used: DNA annealing buffer - 10 mM Tris, pH 8.0, 1 mM EDTA, and 100 mM NaCl; Buffer A - 10 mM Tris, pH 8.0, and 50 mM NaCl; B4 buffer - 10 mM Tris, pH 8.0, and 1 mM EDTA. The imaging buffer was B4 with the addition of NaCl 500 mM. In fluorescence lifetime PAINT, the imaging buffer was phosphate-buffered saline (PBS) with 500 mM NaCl.

Wide-field and confocal FL-SMLM Data Analysis

The image analysis of wide-field and confocal FL-SMLM data was done using the custom-written MATLAB software.^{S1,S2,S5} Initially, an intensity image was generated from the raw photon data by rejecting photons arriving outside 10 ns time gate starting from 0.25 ns after maximum intensity. The resulting intensity image was used for identifying single molecules using a wavelet algorithm.^{S6} All photons within a 3×3 pixel region around the center position of each detected molecule were collected and used for localizing the emitter. And corresponding intensity time trajectories and TCSPC curves for each single molecule were extracted from the raw data. The lifetime values were determined by tail-fitting TCSPC curves with cut-off after 0.3 ns from the peak maximum. For the lifetime fit, we used a mono-exponential decay and minimized the negative log-likelihood function using a Nelder-Mead simplex algorithm.^{S4,S7} TCSPC curves with less than 100 photons in the tail were excluded from the analysis. The obtained lifetime histograms were fitted with a single-Gaussian function using a Nelder-Mead simplex algorithm. Then, intensity-weighted FLIM images were generated.

MIET-SMLM Data Analysis

For MIET experiment data analysis, the lifetimes were converted into heights using the theoretical MIET model.^{S8,S9} For the conversion, three input parameters were required: lifetime of a fluorophore away from coverslip (free-space lifetime), fluorophore quantum yield, and its emission spectra. Using literature values for refractive indices of gold and titanium literature^{S10} and given the sample geometry, lifetime-height dependency (MIET curve) was calculated for the Cy3B fluorophore. Its emission wavelength of 571 nm and the quantum yield of 0.8 were used for calculation. We assumed random orientation of the emission dipole, as the C6 linker was used between a fluorophore and DNA.

FL-SMLM images of single surface-immobilized molecules

Exemplary FL-SMLM images of different fluorophores types are shown in Figure S2. The top row depicts the wide-field FL-SMLM images, while the bottom row depicts the confocal FL-SMLM images.

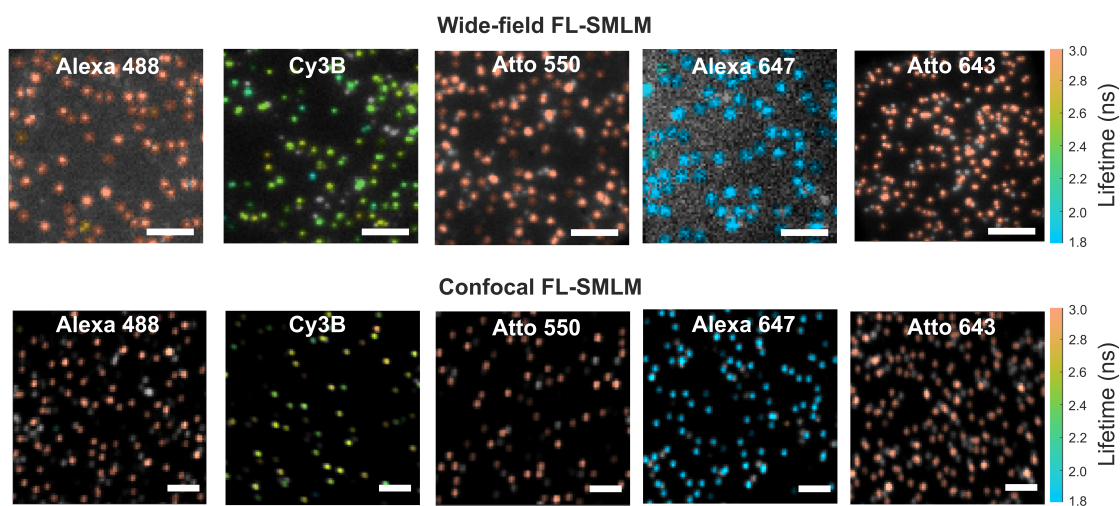


Figure S2: FL-SMLM images of single molecules immobilized on glass surface. Five different types of fluorophores are shown, as indicated on top of each image. Scale bars are 1 μm . The lifetime scale is shown on the right-hand side. Colors represent lifetime values.

Estimation of number of molecules, average lifetimes and average number of photons detected for each fluorophore type before a photobleaching

In this section, we provide the crucial experimental parameters and statistical data: number of molecules analyzed and average lifetimes calculated for each fluorophore type. We also analyzed the intensity time trajectories of single molecules and counted photons detected in each such trajectory, before the photobleaching. The average number of photons for each fluorophore type was calculated for the following fluorophores: Alexa 488, Cy3B, Atto550, Alexa 647, and Atto 643, as listed in Table S1.

Table S1: The number of molecules used in lifetime histograms, average lifetime values with standard deviations, and estimation of average number of photons detected before a photobleaching for different fluorophore types measured with wide-field and confocal FL-SMLM.

Fluorophore	Wide-field N of molecules	Confocal N of molecules	Wide-field τ (ns)	Confocal τ (ns)	Wide-field Photons	Confocal Photons
Alexa 488	594	372	3.24 ± 0.26	3.39 ± 0.37	4711	3541
Cy3B	867	317	2.45 ± 0.13	2.56 ± 0.16	8187	5184
Atto 550	663	732	3.70 ± 0.19	3.83 ± 0.25	12093	9971
Alexa 647	613	586	1.52 ± 0.22	1.47 ± 0.17	933	539
Atto 643	624	290	3.77 ± 0.22	3.83 ± 0.21	13526	4915

Lifetime histograms of Atto 550 and Atto 643 fluorophores

In addition to the fluorophore types displayed in Figure 2 in the main text, we imaged of surface-immobilized Atto 550 and Atto 643 fluorophores using the both wide-field and confocal FL-SMLM. The peaks were fitted with a single-Gaussian function. We found full agreement between the lifetime values obtained using the both techniques, see Figure S3.

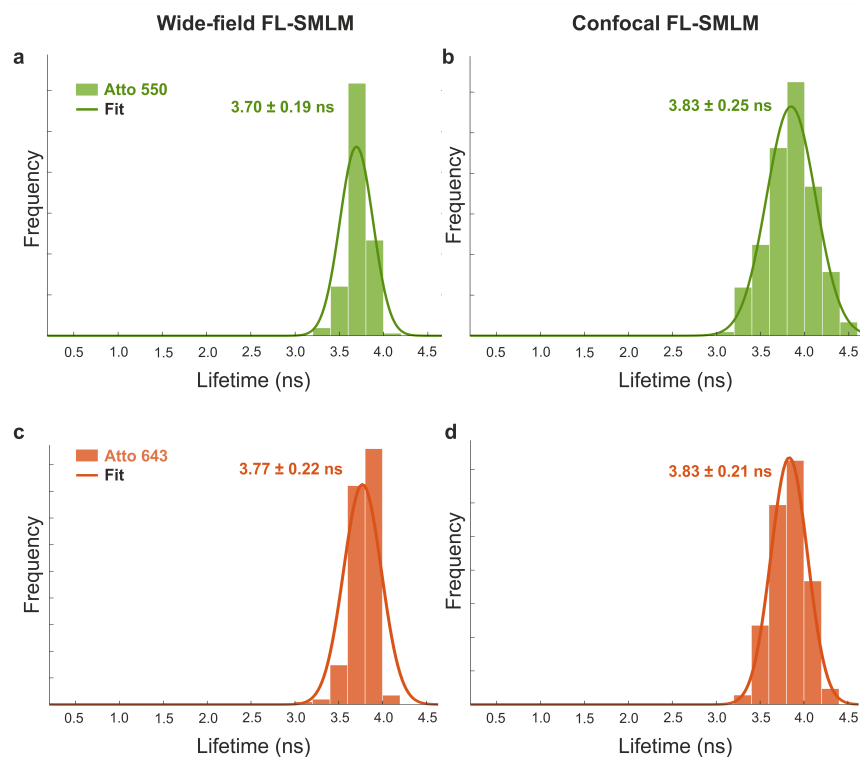


Figure S3: Lifetime histograms of the Atto 550 (a, b) and Atto 643 (c, d), measured using wide-field and confocal FL-SMLM, and the corresponding single-Gaussian fits (solid lines). The average lifetime and standard deviation are given in the plot.

We produced lifetime histograms by accumulating data from several regions of interest (typically 2 to 4 regions were combined together). The number of molecules, utilized in each histogram, is listed in Table S1.

Comparison of fluorescence lifetimes of wide-field and confocal FL-SMLM

We compared the average lifetime values obtained by confocal and wide-field FL-SMLM images for the fluorophores emitting in different spectral regions, see Figure S4. Both techniques show a remarkable agreement for the lifetime data, in different spectral regions.

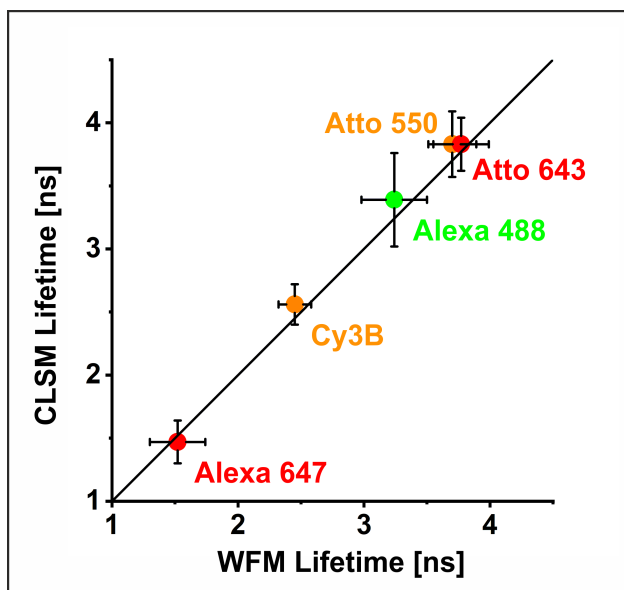


Figure S4: Average lifetimes of Alexa 647 and Atto 643 (far-red emission), Atto 550 and Cy3B (orange emission), and Atto 488 (green emission) for wide-field and confocal FL-SMLM. The fluorophore color depicts the emission wavelength.

MIET-SMLM imaging of surface-immobilized Cy3B fluorophores

We measured the lifetime values of Cy3B fluorophores immobilized on top of SiO₂ spacer with different thicknesses and compared it to the theoretical values calculated by MIET theory.^{S8,S9} We assumed that the actual height of a fluorophore above the gold layer is given by the thickness of SiO₂ spacer combined with the width of the BSA-biotin/Neutravidin layer. A comparison between measured and theoretical lifetime values, as well as measured and theoretical height values are listed in Table S2 and S3. The number of molecules used for the wide-field and confocal MIET-SMLM analysis for each spacer thicknesses are listed in Table S4.

Table S2: Experimental and theoretical lifetime values of single Cy3B fluorophores using MIET-SMLM.

	Wide-field	Confocal
$\tau_{\text{theory}}(\text{ns})$	$\tau_{\text{experiment}}(\text{ns})$	$\tau_{\text{experiment}}(\text{ns})$
1.07	1.14 ± 0.18	1.05 ± 0.25
1.81	1.75 ± 0.13	1.81 ± 0.20
2.18	2.13 ± 0.13	2.13 ± 0.15

Table S3: Experimental and theoretical height values of single Cy3B fluorophores using MIET-SMLM.

	Wide-field	Confocal
$h_{\text{designed}}(\text{nm})$	$h_{\text{experiment}}(\text{nm})$	$h_{\text{experiment}}(\text{nm})$
42	44.01 ± 5.23	42.24 ± 6.72
62	60.35 ± 4.83	62.58 ± 8.06
82	76.30 ± 5.66	77.09 ± 7.26

Table S4: MIET-SMLM experiment: Cy3B fluorophore on top of spacers with different thicknesses. The number of molecules used in lifetime histograms and the average number of detected photons emitted by fluorophores before the photobleaching

Spacer thickness	Wide-field N of molecules	Confocal N of molecules	Wide-field N of photons	Confocal N of photons
Cy3B 30 nm	514	187	517	347
Cy3B 50 nm	485	436	2283	1650
Cy3B 70 nm	593	1057	5233	3566

Exemplary MIET-SMLM images of Cy3B fluorophores immobilized on top of SiO₂ spacers with different thicknesses are shown in Figure S5. The upper panel depicts the wide-field MIET-SMLM images, while the lower panel depicts the confocal MIET-SMLM images.

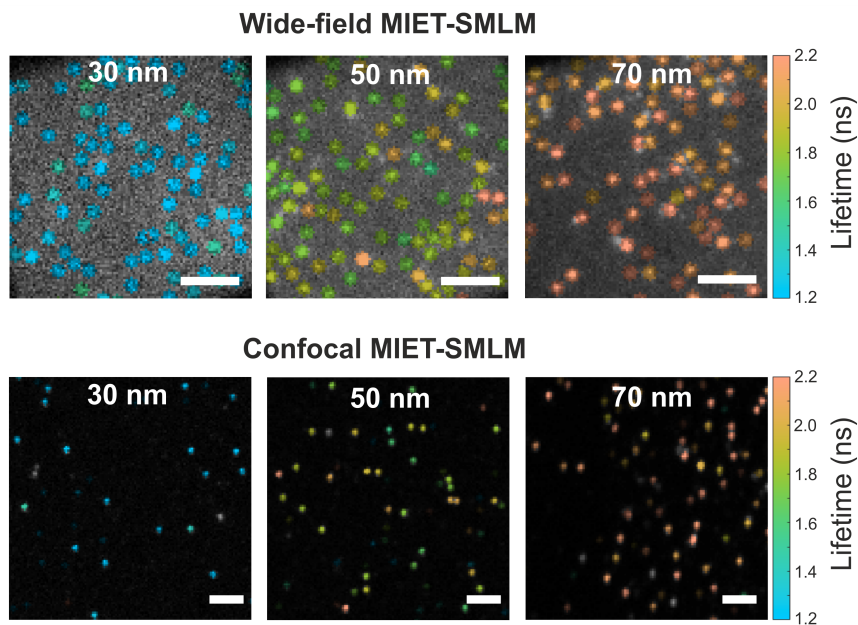


Figure S5: MIET-SMLM images of Cy3B fluorophores on top of a glass/gold/SiO₂ substrate for different values of SiO₂ layer thickness (30, 50, and 70 nm) for wide-field (top) and confocal (bottom) MIET-SMLM measurements. Scale bars are 1 μ m. The lifetime scale is shown on the right-hand side. Colors represent lifetime values.

Comparison of fluorescence lifetimes of wide-field and confocal MIET-SMLM.

We compared the lifetimes and heights obtained on confocal and wide-field microscopes in MIET-SMLM measurements, see Figure S6.

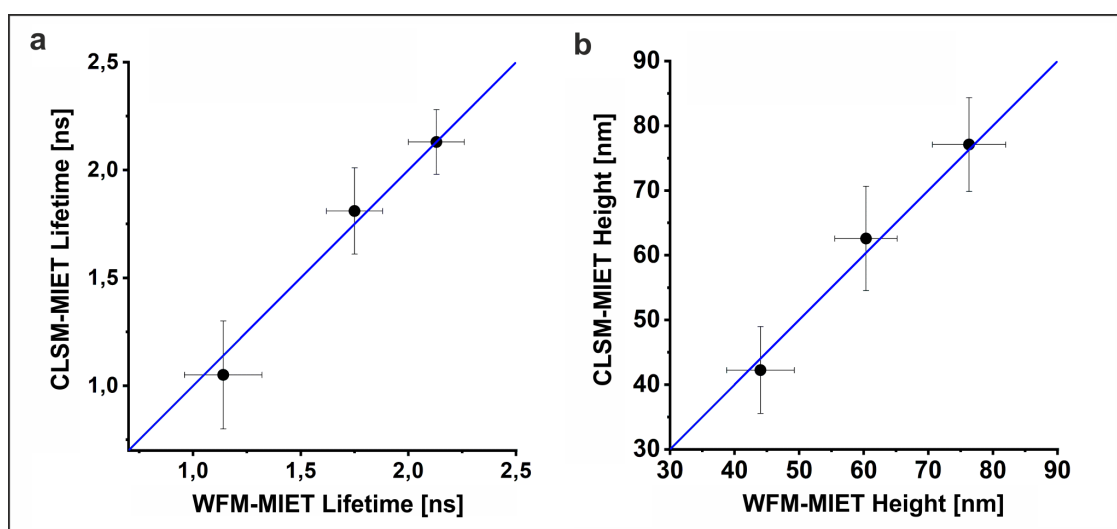


Figure S6: Comparison of average lifetimes (a) and heights (b) for wide-field and confocal MIET-SMLM measurements.

Estimation of lateral localization precision of Cy3B fluorophores in MIET-SMLM experiments

For analysis of lateral localization precision of MIET measurements, TrackNTrace software kit was employed.^{S2} The software is available in free access via link:

<https://github.com/scstein/TrackNTrace>. A spatial binning of 8 pixels and a time bin of 1000 ms were chosen. The detection of molecules was performed using a cross-correlation algorithm and pixel-integrated Gaussian MLE fitting. Localizations with a PSF width of more than 345 nm and a number of photons smaller than 100 were rejected. Localization precision for each spacer thickness was estimated by modified Mortensen’s equation,^{S11,S12} see Table S5.

Table S5: Localization precision of Cy3B fluorophores in MIET-SMLM experiment, for different SiO₂ spacer thickness.

Spacer thickness	Wide-field Loc. precision (nm)	Confocal Loc. precision (nm)
30 nm	17.4	12.4
50 nm	18.4	10.9
70 nm	19.6	11.2

FL-PAINT imaging

Here, we compare the performances of wide-field and confocal FL-PAINT imaging.

Immunolabeling for FL-PAINT imaging

The DNA docking strands (Biomers GmbH, Ulm, Germany) were functionalized with an azide group at the 5'-end. The coupling of the docking strands to the unconjugated nanobodies FluoTag-Q anti-TagBFP (NanoTag Biotechnologies GmbH, Göttingen, Germany, Cat. No: N0501) was performed as described elsewhere.^{S13} Following sequences of imager strands were used (5' to 3'): P1 - CTAGATGTAT, R4 - TGTGTGT, and P3 - GTAATGAAGA. The imagers were purchased labeled from Eurofins Genomics, Germany, modified with Alexa 647, Cy3B or ATTO 550 fluorophores at its 3'-end. It was aliquoted in TE buffer (Tris 10 mM, EDTA 1 mM, pH 8.0) at a concentration of 1 μ M and stored at -20°C . Prior to the experiment, the strands were diluted to the final concentration of 0.2 nM in PBS buffer with NaCl 500 mM. The imager solution (500 μ L) was injected into the chamber.

FL-PAINT data acquisition and analysis

We selected candidates for FL-PAINT imaging of cells based on the expression level of blue fluorescent protein (BFP) and green fluorescent protein (GFP). Specifically, the cells were initially imaged by the following laser excitation wavelengths: BFP - 405 nm and GFP - 488 nm lasers, and using suitable emission filters. Afterwards, we proceeded with FL-PAINT imaging of a selected cell. For both wide-field and confocal FL-PAINT data analysis, custom Matlab software kit TrackNTrace was used.^{S2,S6} The software is available on GitHub via the link:

<https://github.com/scstein/TrackNTrace>. Similar data analysis parameters were used as in the previous study^{S14} and described below.

Wide-field FL-PAINT data analysis

For the wide-field FL-PAINT data analysis, we chose a spatial binning of 8 pixels (corresponding to a virtual pixel size of 192 nm) and a time bin of 500 ms. The detection and precise sub-pixel localization of emitters was performed using a cross-correlation algorithm and pixel-integrated Gaussian MLE fitting. Molecules that were detected in only one frame were discarded. For lifetime determination, we discarded the first 0.1 ns after the maximum of TCSPC curves, and the remaining decay was fitted with a mono-exponential function using a maximum likelihood estimator (MLE). Only lifetime values in the range from 0.5 ns to 5.0 ns were taken into account. Also, localizations with a PSF width of more than 345 nm and a number of photons smaller than 100 were filtered out. After reconstructing a super-resolution image, a drift correction was applied.

Confocal FL-PAINT data analysis

For the confocal FL-PAINT imaging, the following acquisition settings were used: region of interest $25 \times 25 \mu\text{m}^2$, virtual pixel size 100 nm, pixel dwell time 2.5 $\mu\text{s}/\text{pixel}$, and a TCSPC time resolution 16 ps. Five scans were combined together (total time bin of 500 ms) and analyzed by TrackNTrace software. Localizations that appeared in a single frame were discarded. We also filtered out localizations with a PSF width of more than 180 nm or/and a localization with number of photons less than 100. After reconstructing a super-resolution image, a drift correction was applied.

FL-PAINT images resolution estimation and Fourier ring correlation maps

The Fourier ring correlation (FRC) maps were obtained for reconstructed super-resolution images using NanoJ-SQUIRREL ImageJ plugin,^{S15} see Figure S7 a and b, and the average resolutions in far-red spectral region were calculated as 129.7 nm and 77.5 nm for wide-

field FL-PAIN_T and confocal FL-PAIN_T, respectively. For two-target FL-PAIN_T imaging the average resolutions were 69.9 nm and 61.3 nm for wide-field FL-PAIN_T and confocal FL-PAIN_T, correspondingly.

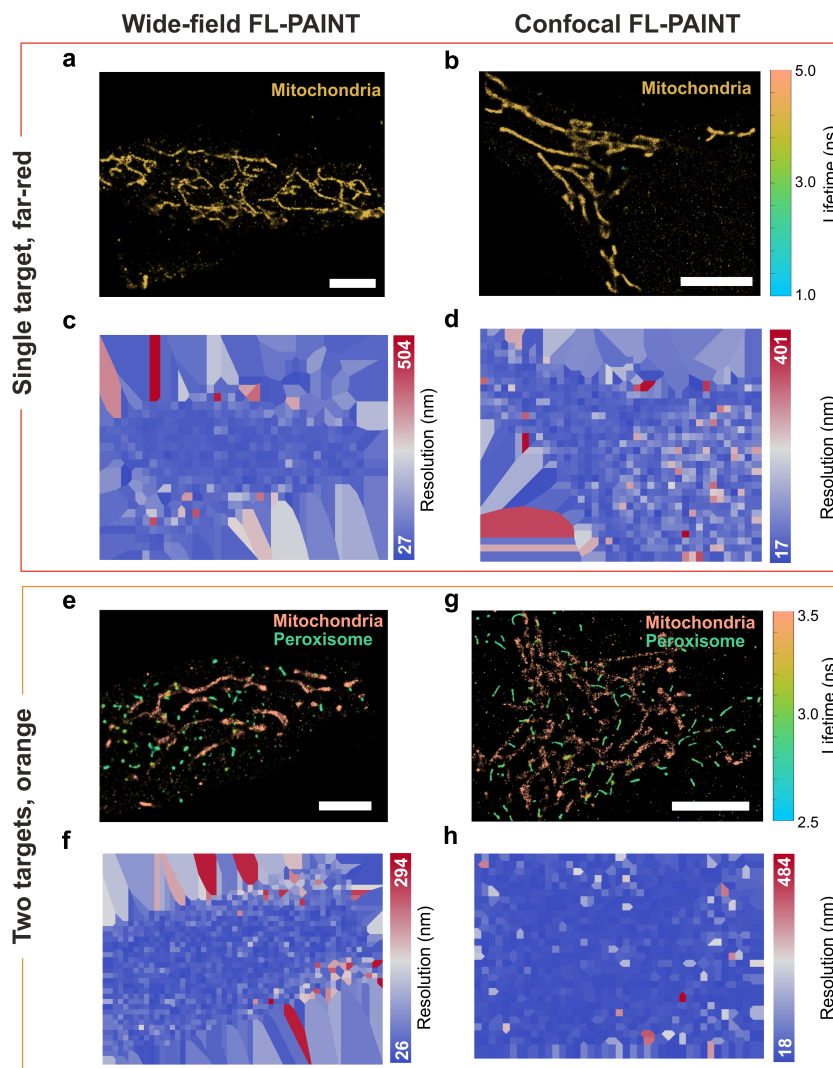


Figure S7: Image resolution estimation and FRC maps. Single-target wide-field (a) and confocal (b) FL-PAIN_T images of mitochondria. Lifetime colorbar is shown on the right-hand side of the images. (c-d) FRC maps of the corresponding super-resolution images from (a-b). The color bar on the right encodes the FRC resolution. Double-target wide-field (e) and confocal (g) FL-PAIN_T images of mitochondria and peroxisomes and corresponding FRC maps (f-h). Scale bars are 5 μ m.

Two-target confocal FL-PAINT in the far-red spectral region

The two fluorophores selected for FL-PAINT imaging in the far-red spectral region are Alexa 647 and Atto 643, with the average lifetimes of 1.5 ns and 3.8 ns correspondingly (for DNA-attached fluorophores). The average localization precision and average resolution for the confocal FL-PAINT image are 11.1 nm and 89.3 nm, with the minimum resolution of 16.2 nm, see Figure S8.

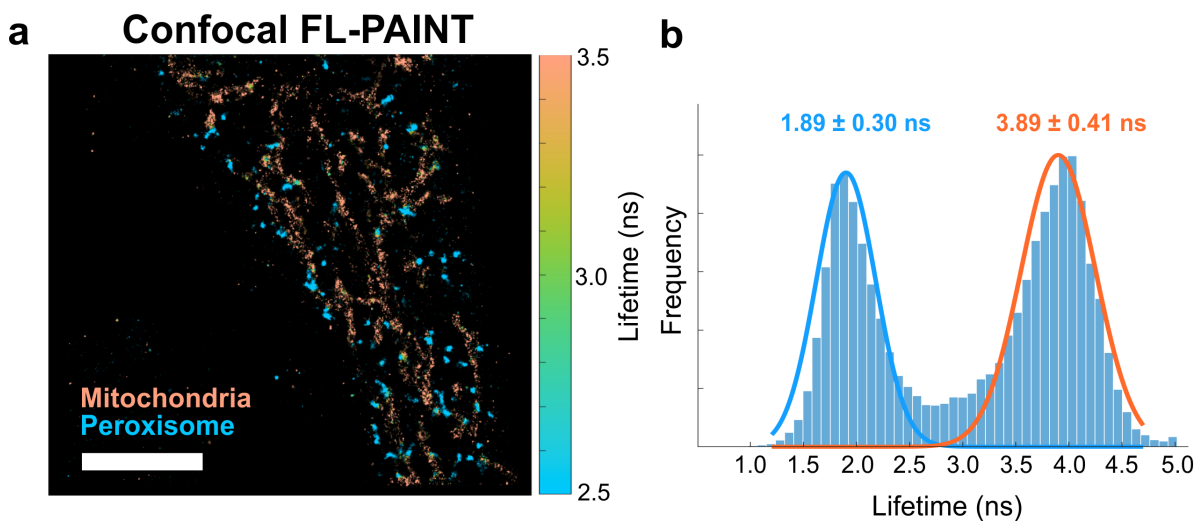


Figure S8: (a) Two-target confocal FL-PAINT imaging in far-red spectral region. Mitochondria and peroxisomes were labeled with imagers P1-Alexa 647 and P3-Atto 643 correspondingly. Lifetime colorbar is shown on the right-hand side of the image. (b) The lifetime histogram with two-Gaussian fit. The average lifetime and standard deviation are shown on the plot. Scale bar is 5 μ m.

Image acquisition speed of wide-field and confocal FL-SMLM and FL-PAINT

To compare the speed at which localization events are accumulated during the wide-field and confocal data acquisition process, we used two different experiments: 1) surface fictionalized with high coverage density of docking strands and a low concentration of imager strand, see Figure S9 a,b and 2) FL-PAINT imaging of fixed HeLa cell with TOMM20 labeled with the docking strand, see Figure S9 c,d.

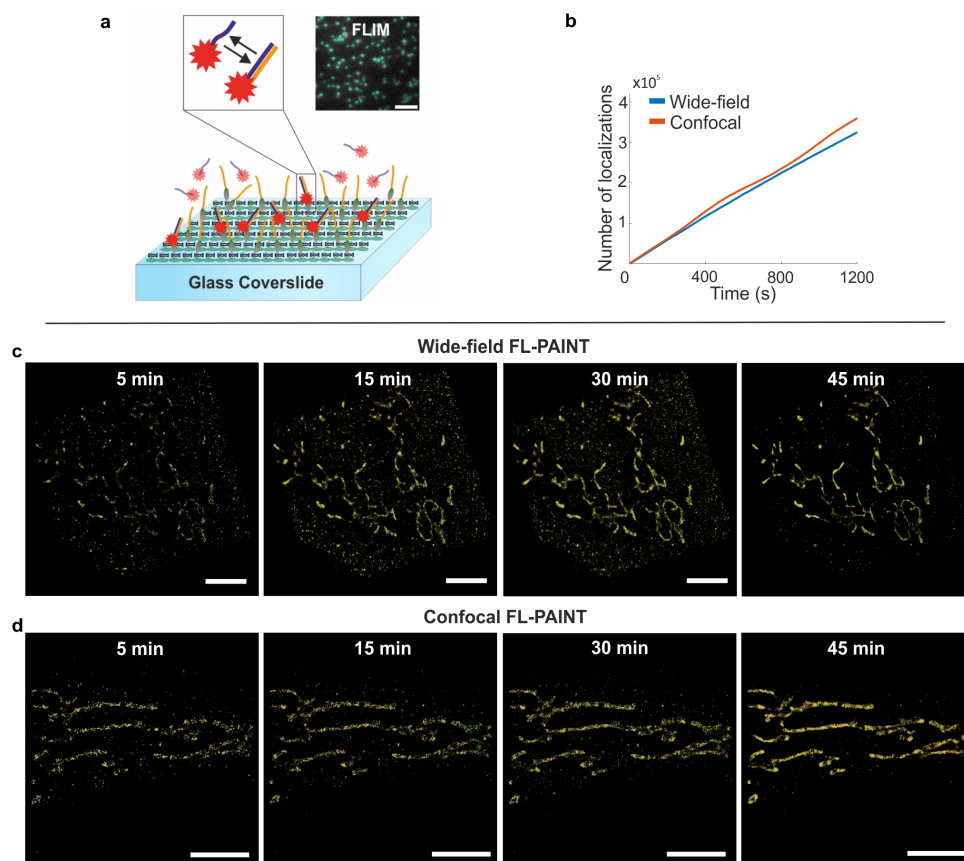


Figure S9: (a) Surface functionalized with docking strands and a solution with the complementary imager strand labeled with Atto 550 fluorophore. Inset on the left - transient binding of imager to docking strand, inset on the right - a single frame of wide-field FL-SMLM. The scale bar is 1 μm . (b) Comparison of number of blinking events registered in the same sample using wide-field and confocal FL-SMLM. (c,d) Qualitative comparison of data accumulation in cellular imaging of mitochondria using wide-field camera (c) and confocal (d) FL-PAINT. Scale bars are 5 μm .

Target crosstalk evaluation in FL-PAINT imaging

In this section, we calculated target crosstalk for the two-target FL-PAINT images shown in Figure 4 in the main text. For the purpose, we fitted the lifetime histograms with two-Gaussian function and manually determined lifetime threshold values to separate between the two different targets. We calculated the total crosstalk as the total number of localizations in-between thresholds (wrong attribution), divided by the total number of localizations beyond thresholds (correct attribution), as shown in Figure S10.

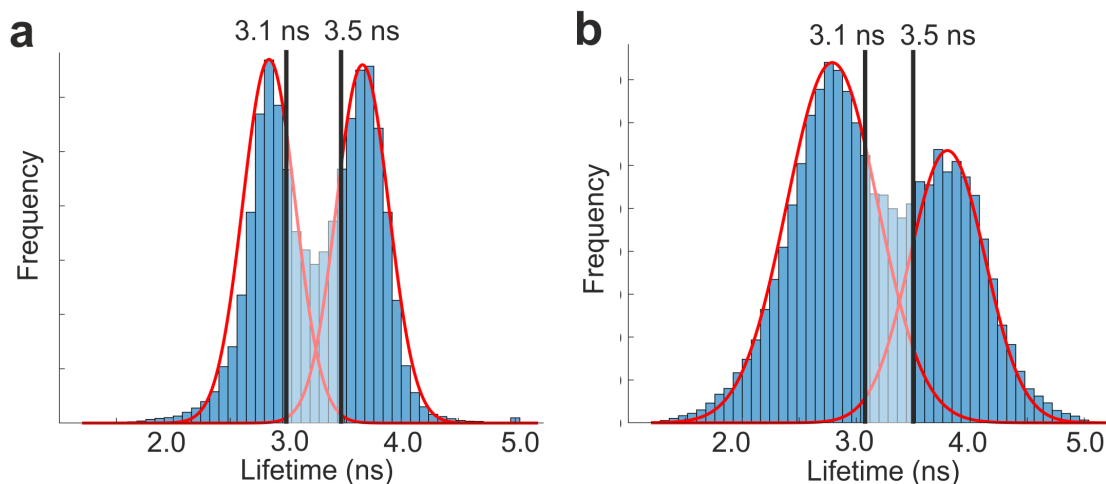


Figure S10: Target crosstalk evaluation in FL-PAINT. Lifetime distribution histograms with the fit of two Gaussians (red curves) are shown. Crosstalk is calculated based on lifetime threshold values (black solid lines). To improve the separation between the targets, localizations in-between two lifetime threshold values were excluded (histogram regions marked in light blue color). (a) Lifetime histogram and targets separation of HeLa cell image from Figure 4e – two-target total crosstalk 1.3%; (b) Lifetime histogram and targets separation of HeLa cell image from Figure 4g – two-target total crosstalk 3.1%

References

- (S1) Oleksiievets, N.; Thiele, J. C.; Weber, A.; Gregor, I.; Nevskiy, O.; Isbaner, S.; Tsukanov, R.; Enderlein, J. Wide-Field Fluorescence Lifetime Imaging of Single Molecules. *The Journal of Physical Chemistry A* **2020**, *124*, 3494–3500.
- (S2) Thiele, J. C.; Helmerich, D. A.; Oleksiievets, N.; Tsukanov, R.; Butkevich, E.; Sauer, M.; Nevskiy, O.; Enderlein, J. Confocal Fluorescence-Lifetime Single-Molecule Localization Microscopy. *ACS Nano* **2020**, *14*, 14190–14200.
- (S3) Gordon, M. P.; Ha, T.; Selvin, P. R. Single-molecule high-resolution imaging with photobleaching. *Proceedings of the National Academy of Sciences* **2004**, *101*, 6462–6465.
- (S4) Isbaner, S.; Karedla, N.; Kaminska, I.; Ruhlandt, D.; Raab, M.; Bohlen, J.; Chizhik, A.; Gregor, I.; Tinnefeld, P.; Enderlein, J., et al. Axial colocalization of single molecules with nanometer accuracy using metal-induced energy transfer. *Nano letters* **2018**, *18*, 2616–2622.
- (S5) Thiele, J. C.; Nevskiy, O.; Helmerich, D. A.; Sauer, M.; Enderlein, J. Advanced Data Analysis for Fluorescence-Lifetime Single-Molecule Localization Microscopy. *Frontiers in Bioinformatics* **2021**, *1*, 56.
- (S6) Stein, S. C.; Thiart, J. TrackNTrace: A simple and extendable open-source framework for developing single-molecule localization and tracking algorithms. *Sci. Rep.* **2016**, *6*, 37947.
- (S7) Gregor, I.; Chizhik, A.; Karedla, N.; Enderlein, J. Metal-induced energy transfer. *Nanophotonics* **2019**, *8*, 1689–1699.
- (S8) Enderlein, J. Single-molecule fluorescence near a metal layer. *Chemical Physics* **1999**, *247*, 1–9.

- (S9) Chizhik, A. I.; Rother, J.; Gregor, I.; Janshoff, A.; Enderlein, J. Metal-induced energy transfer for live cell nanoscopy. *Nature Photonics* **2014**, *8*, 124.
- (S10) Rakić, A. D.; Djurišić, A. B.; Elazar, J. M.; Majewski, M. L. Optical properties of metallic films for vertical-cavity optoelectronic devices. *Appl. Opt.* **1998**, *37*, 5271–5283.
- (S11) Mortensen, K. I.; Churchman, L. S.; Spudich, J. A.; Flyvbjerg, H. Optimized localization analysis for single-molecule tracking and super-resolution microscopy. *Nature Methods* **2010**, *7*, 377–381.
- (S12) Rieger, B.; Stallinga, S. The lateral and axial localization uncertainty in super-resolution light microscopy. *ChemPhysChem* **2014**, *15*, 664–670.
- (S13) Sograte-Idrissi, S.; Oleksiievets, N.; Isbaner, S.; Eggert-Martinez, M.; Enderlein, J.; Tsukanov, R.; Opazo, F. Nanobody detection of standard fluorescent proteins enables multi-target DNA-PAINT with high resolution and minimal displacement errors. *Cells* **2019**, *8*, 48.
- (S14) Oleksiievets, N.; Sargsyan, Y.; Thiele, J. C.; Mougios, N.; Sograte-Idrissi, S.; Nevskiy, O.; Gregor, I.; Opazo, F.; Thoms, S.; Enderlein, J.; Tsukanov, R. Fluorescence lifetime DNA-PAINT for multiplexed super-resolution imaging of cells. *Communications Biology* **2022**, *5*, 1–8.
- (S15) Culley, S.; Albrecht, D.; Jacobs, C.; Pereira, P. M.; Leterrier, C.; Mercer, R., Jason andHenriques Quantitative mapping and minimization of super-resolution optical imaging artifacts. *Nature Methods* **2018**, *15*, 263–266.